Nonlinear Raman spectroscopy of the low-lying levels of the Sm^{2+} ion doped in SrF_2 and CaF_2 crystals

2001 J. Phys.: Condens. Matter 13 735

(http://iopscience.iop.org/0953-8984/13/4/319)

INSTITUTE OF PHYSICS PUBLISHING JOURNAL OF PHYSICS: CONDENSED MATTER

J. Phys.: Condens. Matter **13** (2001) 735–741 www.iop.org/Journals/cm PII: S0953-8984(01)17846-X

Nonlinear Raman spectroscopy of the low-lying levels of the Sm^{2+} ion doped in SrF_2 and CaF_2 crystals

V Aarstrand[1], T Fotteler[1], W Beck[1], D Ricard[1,3] and J-C Gâcon[2]

[1] Laboratoire d'Optique Quantique, Ecole Polytechnique, 91128 Palaiseau Cedex, France
[2] Laboratoire de Physico-Chimie des Matériaux Luminescents, UMR 5620 CNRS, Université Lyon-I, 69622 Villeurbanne Cedex, France

E-mail: daniel.ricard@lac.u-psud.fr

Received 9 October 2000, in final form 23 November 2000

Abstract

We used coherent anti-Stokes Raman scattering (CARS) spectroscopy to study the symmetry of the low-lying levels of the Sm^{2+} ion doped in sites of cubic (O_h) symmetry in the SrF_2 and CaF_2 matrices. Taking advantage of the polarization sensitivity of the Raman spectroscopic techniques, we confirm that the line at $\approx$652 cm^{-1} (that we could only observe in the SrF_2 case because of wavelength limitations) corresponds to excitation from the ground ($4f^6\ ^7F_0$) A_{1g} level to the Stark T_{2g} level originating from the splitting of the ($4f^6\ ^7F_2$) multiplet. In the same SrF_2 sample, the ($4f^6$) $^7F_0 \rightarrow\ ^7F_1$ transition was observed to be weaker. In CaF_2 matrices in which it is more easily detected, we checked its T_{1g} symmetry

1. Introduction

Two-photon transitions allow one to access energy levels that often cannot be reached using one-photon transitions [1]. For example, Raman spectroscopy has proven a powerful technique for the study of low-lying excited levels. It may be performed in several ways, spontaneous Raman scattering being the 'oldest' one. In the nonlinear Raman spectroscopic techniques [2], a 'laser' beam of frequency ω_1 and a 'Stokes' one of frequency ω_2 copropagate in the medium. In the Raman gain technique, the gain experienced by the weak 'Stokes' beam is measured. In inverse Raman spectroscopy, the attenuation experienced by the weak 'laser' beam is monitored. In coherent anti-Stokes Raman spectroscopy (CARS), the intensity of the beam generated at the 'anti-Stokes' frequency $\omega_3 = 2\omega_1 - \omega_2$ is measured. In coherent Stokes Raman spectroscopy (CSRS), one monitors the intensity of the 'second Stokes' beam generated at frequency $\omega_4 = 2\omega_2 - \omega_1$. All these techniques are equivalent in principle, but practical considerations may make some or one of them more suitable.

Transition-metal or rare-earth ions are systems that can be studied using Raman techniques [3]. We concentrate here on the Sm^{2+} ion doped in alkaline-earth fluorides, SrF_2 and

[3] Corresponding author. Present address: Laboratoire Aimé Cotton, Université Paris-Sud, Bâtiment 505, 91405 Orsay Cedex, France.

0953-8984/01/040735+07$30.00

CaF_2. These systems, in which the Sm^{2+} ions occupy sites of cubic (O_h) symmetry, have been extensively studied [4, 5] mainly using absorption and luminescence techniques, sometimes in the presence of a magnetic field. As is generally the case for the 4f electrons of rare-earth ions, for the Sm^{2+} ion of ground configuration $[Xe]4f^6$, the crystal field effect is small compared with spin–orbit and Coulomb interactions. Due to the large energy difference between the ground ^7F term, on which we concentrate, and the higher ones, the L–S coupling scheme provides a good starting point as indicated by the coefficients of fractional parentage [6]. For the free ion, the first levels in order of increasing energy are then, to a good degree of accuracy, $^7F_0$, $^7F_1$, $^7F_2$, ... When embedded in the fluoride crystals, the $^7F_2$ multiplet is split into two Stark levels of E_g and T_{2g} symmetry, whereas the degeneracy of the $^7F_1(T_{1g})$ level is not lifted. Although Zeeman splitting measurements [5, 7] as well as theoretical predictions [8] have shown that the $^7F_2(T_{2g})$ level lies lower than the $^7F_2(E_g)$ one, the opposite was sometimes reported without any experimental evidence [9]. Using the polarization sensitivity of Raman measurements, we confirm here the first assignment.

2. Theory

In CARS spectroscopy, keeping only the terms involving the Raman resonance $\omega_{eg} \approx \omega_1 - \omega_2$ where g and e are the ground and excited states respectively, the amplitude of the generated wave is proportional to the effective susceptibility:

$$\chi_{eff}^{(3)CARS} = \sum_{\alpha,\beta,\gamma,\delta} e_{AS}^{\alpha} e_L^{\beta} e_L^{\gamma} e_S^{\delta} \chi_{\alpha\beta\gamma\delta}^{(3)CARS}(\omega_3; \omega_1, \omega_1, -\omega_2) \tag{1}$$

where e_L for example is the unit vector defining the polarization of the laser beam and

$$\chi_{\alpha\beta\gamma\delta}^{(3)CARS}(\omega_3; \omega_1, \omega_1, -\omega_2) = \frac{1}{2}\left(\frac{R_{\beta\alpha}^*(\omega_3) R_{\delta\gamma}(\omega_1)}{\varepsilon_0 \hbar(\omega_{eg} - \omega_1 + \omega_2 - i\Gamma_{eg})} + \beta \leftrightarrow \gamma\right) \tag{2}$$

the second term inside the parentheses being obtained by interchanging the β and γ indices. In Raman gain spectroscopy, the gain at the Stokes frequency ω_2 is proportional to the imaginary part of a similar susceptibility, to which the Raman (Stokes) cross section is closely related in the case of spontaneous Raman scattering.

The polarization sensitivity of the Raman techniques is due to the tensorial nature of the corresponding susceptibility. In the expression above, away from any intermediate resonance and at low temperature, the Raman tensor **R** is given by:

$$R_{lk}(\omega) = \sum_n \left(\frac{\langle e|d_l|n\rangle\langle n|d_k|g\rangle}{\hbar(\omega_{ng} - \omega)} + \frac{\langle e|d_k|n\rangle\langle n|d_l|g\rangle}{\hbar(\omega_{ne} + \omega)}\right) \tag{3}$$

with d_l the lth component of the electric dipole moment operator and the summation over n being extended to all possible intermediate states. In equation (3), the detuning $\omega_{ng} - \omega$ was assumed to be large compared with the line width Γ_{ng}. The Raman tensors corresponding to the (symmetric) A_{1g}, E_g and T_{2g} and to the (anti-symmetric) T_{1g} representations of the O_h group are easily obtained [10]. As is clear from equation (3), when there is a state, or a group of (possibly degenerate) states, n_0 such that $\omega_{n_0 g}$ is not too different from ω (the detuning being still large compared with the line width), the susceptibility is resonantly enhanced. This resonance enhancement plays an important role in the case of rare-earth ions because of their weak Raman cross sections [11].

3. Experiment

The results we report or discuss here were obtained using Sm-doped SrF_2 and CaF_2 crystals grown using the Bridgman technique under an argon atmosphere. Some of the CaF_2 crystals

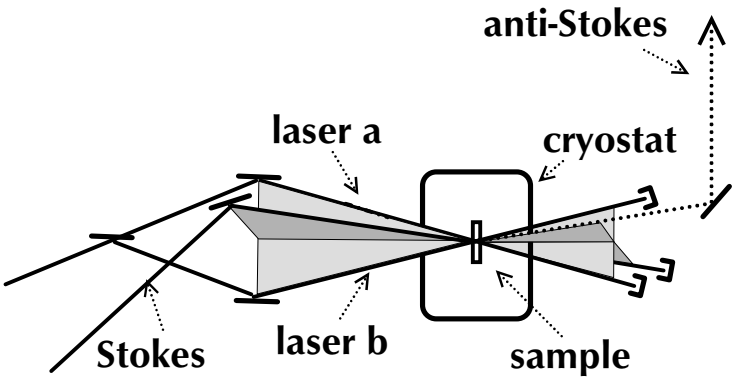

Figure 1. Simplified scheme of the non-coplanar BOXCARS geometry we used in this work.

we used spontaneously contained divalent Sm^{2+} ions and were green. Some of the CaF_2 samples as well as the SrF_2 one were initially transparent and, in order to reduce part of the Sm ions from the trivalent state to the divalent one, they were irradiated by γ-rays from a ^{60}Co source (10 Mrad dose). Upon irradiation, these samples turned green in the CaF_2 case and blue in the SrF_2 one. They were then orientated and cut as parallelepipeds with the edges parallel to the conventional X, Y and Z cubic axes. The nominal Sm concentration was in the 0.5 to 0.1% range for the CaF_2 samples and 0.2% for the SrF_2 one. The Sm^{2+} concentration was typically 100 to 200 times smaller. In the CaF_2 case, it was deduced from the room-temperature absorbance of the samples at ∼620 nm [12]. In the SrF_2 one, it was obtained from the integrated absorbance for the first allowed $(4f^6\ ^7F_0)A_{1g} \rightarrow (4f^5 5d)T_{1u}$ transition at 658 nm, assuming its oscillator strength to be the same as that of the corresponding line (at 690 nm) in CaF_2.

The Sm^{2+} concentration being small, the Raman gain and inverse Raman techniques could not be used in our samples. We used the CARS technique that provides a collimated beam whose direction is determined by phase matching. The corresponding susceptibility was enhanced by choosing an anti-Stokes frequency ω_3 that was smaller but not too remote from the frequency of the aforementioned first allowed $(4f^6\ ^7F_0)A_{1g} \rightarrow (4f^5 5d)T_{1u}$ transition. In the case of CSRS, in order to get the same enhancement, one would have to choose the laser frequency ω_1 close to the aforementioned transition. This cannot be done since, when irradiated by an intense laser beam, bleaching of the sample (due to photo-ionization of Sm^{2+} ions) takes place [13]. This would also be the case for spontaneous Stokes scattering. We could have a resonance enhancement (without bleaching problems) in the case of anti-Stokes spontaneous scattering but the populations of the excited levels are extremely weak at ≈9 K.

In our measurements, the tunable ω_1 and ω_2 beams were generated by two (Continuum ND6000) nanosecond dye lasers pumped by the same frequency-doubled Q-switched Nd:YAG laser. The repetition rate was 50 pulses per second, the pulse duration 5 ns. The dye laser spectral width was 0.05 cm^{-1}. The laser beam was gently focused on the sample with a beam waist of ≈100 μm diameter. The typical peak intensity was 250 MW cm^{-2} for each of the incoming beams. The sample was sitting in a cryo-refrigerator at a temperature of ≈9 K. We used the BOXCARS configuration [14] in a non-coplanar geometry as shown in figure 1. The two 'laser' beams (a and b) propagating in a horizontal plane and the 'Stokes' beam propagating downwards in a vertical plane intersect in the sample. This allows for phase matching of the four-wave mixing process as well as for geometrical separation of the weak

'anti-Stokes' beam, propagating upwards in the vertical plane, from the incident beams. The external angle between each beam and the normal to the input and output sample faces (the Z axis) was typically 20 mrad, so that the four beams nearly propagated along the Z axis. We blocked the incident beams after the sample and sent the anti-Stokes beam through a (ISA U1000) double monochromator to a photomultiplier tube (PMT). The output of this PMT was sent to a boxcar integrator and crudely normalized by dividing it by the laser pulse energy, then averaged over 50 laser shots.

The wavelength of the A_{1g}–T_{1u} transition and the maximum wavelength our tunable dye laser can generate (740 nm) set limitations on the excitation energy range we can study. In the CaF_2 case, choosing the value 694 nm for $\lambda_3 = 2\pi c/\omega_3$, the maximum excitation energy we can reach is ~440–445 cm^{-1}. In the SrF_2 one, with $\lambda_3 = 662$ nm, this maximum excitation energy is ~790–795 cm^{-1}.

4. Results

From the data reported in [5], the $^7F_2(T_{2g})$ and $^7F_2(E_g)$ levels are respectively located at 652 and 1035 cm^{-1} above the $^7F_0(A_{1g})$ ground level in SrF_2. We first discuss the case of the ≈652 cm^{-1} line. The anti-Stokes frequency ω_3 was held constant while the laser (ω_1) and Stokes (ω_2) frequencies were scanned. The polarization of 'laser' beams a and b was set along X and that of the Stokes and anti-Stokes ones both either along Y or along X. The signals we get are displayed in figure 2. They originate then from the $\chi^{(3)}_{YXXY}$ component of the susceptibility tensor in the first case (figure 2(a)) and the $\chi^{(3)}_{XXXX}$ component in the second one (figure 2(b)). As is usually the case in CARS spectroscopy [15], besides the Raman susceptibility given in equation (1), a non-resonant real term mainly originating here in the strontium fluoride matrix also contributes to the anti-Stokes signal. We therefore fitted the resonance that may be seen in figure 2(a) by the modulus squared of

$$A + B\frac{\Gamma}{\omega_0 - \omega' - i\Gamma} \tag{4}$$

with ω_0 the transition frequency, Γ the half-width of the line and $\omega' = \omega_1 - \omega_2$. A and B are real parameters, proportional to the 'magnitude' of the non-resonant and Raman terms respectively. The fit gave us the values $\omega_0/2\pi c \approx 652.6$ cm^{-1} and $\Gamma/2\pi c \approx 0.80$ cm^{-1}.

The resonance is clearly visible in figure 2(a) but is not seen in figure 2(b), indicating that the excited level lying ≈653 cm^{-1} above the ground state is of T_{2g} (and not E_g) symmetry in agreement with previous reports [5, 7, 8]. We note that in the case of the $^5D_2$ multiplet the reverse order was observed [1], which shows that the crystal field model used in [8] fails in reproducing the splitting of the lowest ^5D term.

Because of the aforementioned wavelength limitations, this 653 cm^{-1} transition could not be studied in the case of a CaF_2 host matrix. Likewise, the 1035 cm^{-1} resonance could not be studied in either the CaF_2 or SrF_2 samples. When working far away from any intermediate resonance, the Unsöld (or closure) approximation may be used, leading to a symmetric Raman tensor [16] as is clear from equation (3). The transitions of T_{1g} symmetry are then forbidden; generally, they are expected to be much weaker than the A_{1g}, E_g or T_{2g} ones. Figure 3 that shows a scan about 260 cm^{-1} for the SrF_2:Sm^{2+} sample with the same polarization configuration as in figure 2(a) illustrates this fact. We do not see the $^7F_0(A_{1g}) \rightarrow {}^7F_1(T_{1g})$ transition whereas the $^7F_0(A_{1g}) \rightarrow {}^7F_2(T_{2g})$ one is clearly visible. The rising signal in figure 3 corresponds to the wing of the 290 cm^{-1} optical phonon line of the SrF_2 matrix.

In CaF_2 however, the $^7F_0$–$^7F_1$ line of Sm^{2+} was observed at ≈256 cm^{-1}. Some of our results have already been published [13]. In the present work, using various polarization

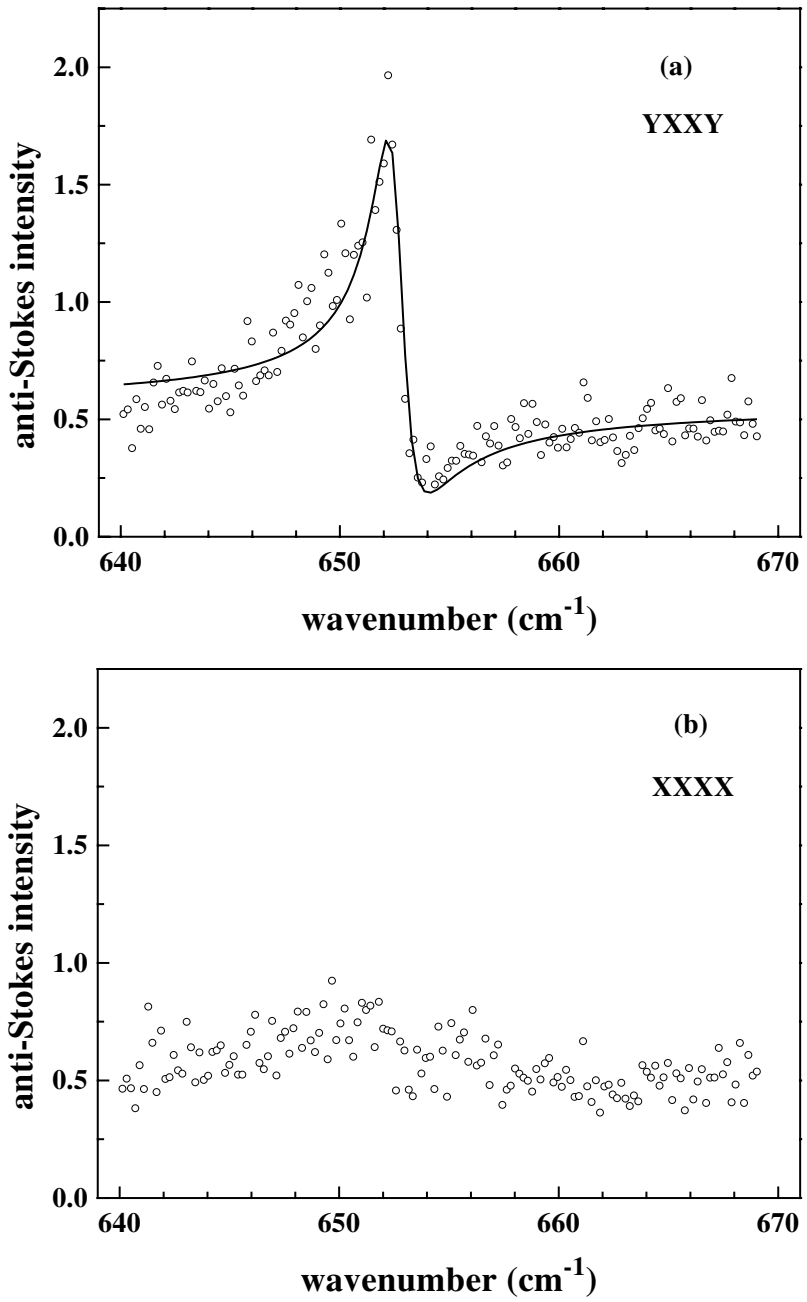

Figure 2. Intensity of the 'anti-Stokes' beam as a function of the wave-number difference $(\omega_1 - \omega_2)/2\pi c$ around 652 cm^{-1} for two different polarization configurations (a) $YXXY$ and (b) $XXXX$. The four indices correspond to the polarization of the anti-Stokes, laser a, laser b and Stokes beams respectively. The sample is SrF_2:Sm^{2+}.

schemes, for example $e_L = e_S = e_{AS} = (1/\sqrt{2}, 1/\sqrt{2}, 0)$ or $e_L = (1/\sqrt{2}, 1/\sqrt{2}, 0)$ and $e_S = e_{AS} = (-1/\sqrt{2}, 1/\sqrt{2}, 0)$, we checked that this transition is of T_{1g} symmetry whereas

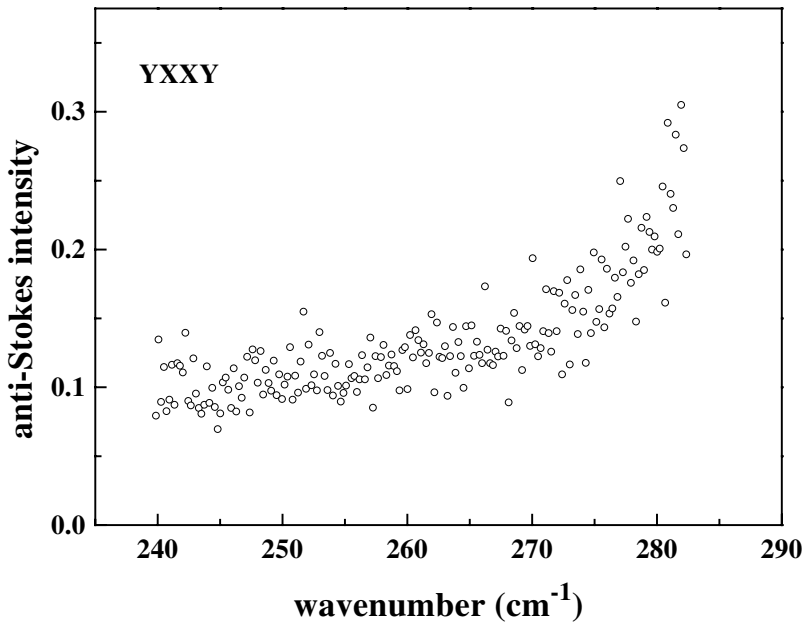

Figure 3. Same as figure 2(a) but for a scan around 260 cm^{-1}.

the optical phonon is T_{2g}. The strength of this 256 cm^{-1} line in CaF_2 is somewhat surprising since, despite the resonance enhancement due to the $(4f^5 5d)T_{1u}$ level (at 690 nm) [17], when summing over the three states that constitute this T_{1u} level, the Raman tensor should remain symmetric. We recall that we could not study the $^7F_0(A_{1g}) \rightarrow {}^7F_2(T_{2g})$ transition in the CaF_2 case.

Acknowledgment

The authors would like to thank J M Dolo who kindly took care of the γ-ray irradiation of our SrF_2 sample.

References

[1] Gâcon J-C, Burdick G W, Moine B and Bill H 1993 *Phys. Rev.* B **47** 11 712
[2] Shen Y R 1984 *The Principles of Nonlinear Optics* (New York: Wiley)
[3] Koningstein J A 1973 *Ann. Rev. Phys. Chem.* **24** 121
Downer M C 1989 *Laser Spectroscopy of Solids II* ed W M Yen (Berlin: Springer) p 29
[4] Feofilov P P and Kaplyanskii A A 1962 *Opt. Spectrosc.* **12** 272
[5] Wood D L and Kaiser W 1962 *Phys. Rev.* **126** 2079
[6] Ofelt G S 1963 *J. Chem. Phys.* **38** 2171
[7] Gerlovin I Ya, Ignat'ev I V and Ovsyankin V V 1999 *Opt. Spectrosc.* **86** 881
[8] Druzhinin V V and Khaimenov A P 1966 *Opt. Spectrosc.* **20** 176
[9] Couto R M and Nicola J H 1986 *J. Phys. C: Solid State Phys.* **19** 7315
[10] Cardona M 1982 *Light Scattering in Solids II* ed M Cardona and G Güntherodt (Berlin: Springer) p 49
[11] Williams G M, Becker P C, Conway J C, Edelstein N, Boatner L A and Abraham M M 1989 *Phys. Rev.* B **40** 4132
[12] Kaiser W, Garrett C G B and Wood D L 1961 *Phys. Rev.* **123** 766
[13] Beck W, Ricard D and Flytzanis C 1996 *Appl. Phys. Lett.* **69** 3197

[14] Eckbreth A C 1978 *Appl. Phys. Lett.* **32** 421
[15] Levenson M D, Flytzanis C and Bloembergen N 1972 *Phys. Rev.* B **6** 3962
[16] Sonnich Mortensen O and Koningstein J A 1968 *J. Chem. Phys.* **48** 3971
[17] Beck W, Fedorov V V, Ricard D, Flytzanis C and Basiev T T 1998 *J. Luminesc.* **79** 241